Applied Soft Computing Journal 89 (2020) 106105

Contents lists available at ScienceDirect

Applied Soft Computing Journal

journal homepage: www.elsevier.com/locate/asoc

Multi-objective railway alignment optimization considering costs and environmental impacts

Hong Zhang [a,b], Hao Pu [a,b,*], Paul Schonfeld [c], Taoran Song [a,b], Wei Li [a,b], Jie Wang [d], Xianbao Peng [e], Jianping Hu [f]

[a] College of Civil Engineering, Central South University, Changsha 410075, China
[b] National Engineering Laboratory for High Speed Railway Construction, Changsha 410075, China
[c] Department of Civil & Environmental Engineering, University of Maryland, MD 20742, United States
[d] China Railway First Survey and Design Institute Group Co. Ltd, Xi'an, 710043, China
[e] China Railway Siyuan Survey and Design Group Co. Ltd, Wuhan 430063, China
[f] China Railway Eryuan Engineering Group Co. Ltd, Chengdu, 610031, China

A R T I C L E I N F O

Article history:
Received 5 June 2019
Received in revised form 18 December 2019
Accepted 14 January 2020
Available online 20 January 2020

Keywords:
Railway alignment design
Multi-objective optimization
Railway costs
Environmental impacts
Particle swarm optimization

A B S T R A C T

With increasing transportation requirements in mountainous regions, railways are encroaching ever more on environmentally-sensitive areas in those regions. Selecting an economical and eco-friendly railway alignment can effectively minimize negative impacts on mountain environments while also reducing costs. To this end, this paper formulates the alignment design problem as a multi-objective optimization model, which includes both economic and environmental objectives. Two new quantitative indexes for measuring environmental impacts are proposed to reflect the degree of vegetation destruction and soil erosion. A multi-objective optimization method based on the particle swarm optimization (PSO) algorithm is proposed for seeking non-dominated solutions. New update mechanisms for dealing with the multi-objective optimization problem are devised. A local repair algorithm based on a customized crossover operator is designed to save promising alignment alternatives during the search process. Two real-world cases are used to demonstrate the effectiveness of the proposed method. The results show that it can trade off the economic and environmental objectives and bypass all the pre-specified forbidden zones, thus providing designers a set of non-dominated alignment alternatives.

1. Introduction

Railways play an important role in modern transportation. Many studies have sought to develop algorithms which can find the most economical railway alignment considering many factors, such as terrain condition, cost features, and multiple constraints [1,2]. However, since the surrounding environment is also affected by building new railways, environmental impacts are also important factors that should be considered during the railway alignment optimization process.

Especially in mountainous regions, the natural environment is fragile, with lush vegetation and nature reserves. Selecting an eco-friendly alignment may effectively reduce the environmental impacts of railway construction. However, the costs and environmental impacts of a railway may be conflicting. It is difficult to aggregate these two evaluation criteria into one single-objective function and jointly optimize them, especially if they are not measurable in commensurate units. This paper presents our approach to multi-objective railway alignment optimization. The optimization model includes three objectives, i.e., the economic objective of minimizing total costs and two environmental objectives of minimizing vegetation destruction and soil erosion. The solution method for the optimization model is founded upon a customized version of the particle swarm optimization (PSO) algorithm [3], which has been successfully used to solve the railway alignment optimization problem by minimizing costs. The major novelties of this study can be summarized as follows:

(1) A multi-objective optimization model combining economic and environmental objectives is formulated. Two new quantitative indexes for measuring environmental impacts are proposed, reflecting the degrees of vegetation destruction and soil erosion.

(2) A multi-objective optimization method based on particle swarm optimization (PSO) algorithm is proposed to solve the model. New update mechanisms for the PSO algorithm are devised to deal with the multi-objective optimization problem.

(3) A local repair algorithm is designed to save promising alignment alternatives during the optimization process.

* Corresponding author at: College of Civil Engineering, Central South University, Changsha 410075, China.
E-mail address: haopu@csu.edu.cn (H. Pu).

https://doi.org/10.1016/j.asoc.2020.106105
1568-4946/

The remainder of this paper is organized as follows. Section 2 reviews existing alignment optimization studies and summarizes their limitations, through which the research objectives of this study are introduced. Section 3 provides a formal description of the railway alignment optimization problem. Section 4 describes the proposed PSO-based multi-objective optimization method. Section 5 presents two real-world railway cases used to demonstrate the effectiveness of the method. Finally, Section 6 summarizes this work.

2. Literature review

The alignment optimization is a complex problem. It is hard to express the relation among the design variables of the alignment and the optimization objective accurately with an explicit function. The objective function of the alignment optimization problem is nonlinear and non-differentiable [4]. Especially when constraints are considered, the objective function is quite unsmooth and has a multitude of local optima in many dimensions. Since the 1960s many studies have explored this problem and developed methods to solve it.

Studies in this field started with the optimization of single-objective models. Multiple criteria for evaluating the alignments were converted into monetary terms and added to form a single-objective function using the weighted sum method. Many different methods have been developed. Among these methods, the genetic algorithm (GA) is believed to be the most representative one. Jong [5] developed the original highway alignment optimizing method based on GA. In further studies, Kim et al. [6] proposed a hierarchical optimization strategy to improve the computational efficiency. Kang et al. [7] developed a method for prescreening constraints and repairing violated constraints. Lai [8] took the station locations into consideration and developed a concurrent optimization method for rail transit alignments and station locations. Davey et al. [9] extended the optimization model incorporating animal movement and mortality into alignment optimization. Babapour et al. [10] built the model for the forest road profile optimization problem and solved the model with GA. Besides GA, other algorithms also archived good performances at solving the alignment optimization problem. Costa et al. [11,12] introduced the simulated annealing algorithm to optimize the high-speed railway alignment. Hare et al. [13,14] depicted the road profile as a quadratic spline and optimized the vertical alignment by minimizing the earthwork cost. To optimize the horizontal alignment of roads, Mondal et al. [15] developed a bi-level optimization model and used the mesh adaptive direct search (MADS) algorithm to solve the model. Hirpa et al. [16] further developed a bi-objective optimization framework for the three-dimensional road alignment design. Discrete algorithms were used by Pushak et al. [17] to find optimized corridors for highway alignments, the computing efficiency and robustness of five discrete algorithms were analyzed. Li et al. [18] and Pu et al. [19,20] focused on solving the railway alignment optimization problem in complex mountainous regions and developed an optimization method based on the distance transform algorithm. To improve the computing efficiency, Song et al. [21] further developed a parallel distance transform algorithm for railway alignment optimization. These methods can solve the alignment optimization problem effectively so that the comprehensive total costs are minimized.

Despite their success, one important limitation of the approaches mentioned above must be noted. The criteria for evaluating the alignments are not measurable in commensurate units. Converting different evaluation criteria precisely into monetary units can be very difficult, thereby limiting the performance of the approaches mentioned above when multiple evaluation criteria are considered. To overcome this limitation, Maji and Jha [22] proposed a multi-objective alignment optimization method based on a genetic algorithm (GA), in which the considered evaluation criteria (i.e., user cost and construction cost) were not aggregated into one single-objective but optimized separately. Their method [22] can trade off the two different evaluation criteria and provide a set of non-dominated alignment alternatives. However, the environmental impacts, which are increasingly important in modern construction, were not considered in their study. In an extended effort, Maji and Jha [23] added an environmental objective into the optimization model, in which the total impacted area of environmentally-sensitive regions was used as the quantitative index. Yang et al. [24] further improved the method by incorporating preference information in the optimization process.

However, these GA-based methods for alignment optimization still have a notable limitation, namely that "the optimization result depends on the distribution of preset cutting planes, on which the points of intersection (PIs) are located. [18]" Setting the distribution for the PIs appropriately is a difficult problem. To overcome this problem, Li et al. [18] developed a hybrid optimization method based on a distance transform (DT) algorithm and a genetic algorithm (GA), in which the DT algorithm automatically sets cutting planes before the GA refines the alignment. Nevertheless, another limitation remains, i.e., the PIs are restricted to the cutting planes. Some valuable PIs may be missed, thereby limiting the quality of the resulting alignment.

Particle swarm optimization (PSO), proposed by Eberhart and Kennedy [25], is an evolutionary algorithm designed for solving continuous optimization problems [3] and has been used to solve many real-world problems (e.g., reservoir flood control operation [26], gate assignment [27]). Shafahi and Bagherian [28] first introduced PSO for solving the alignment optimization problem and developed a customized PSO algorithm. However, the approach proposed by Shafahi and Bagherian [28] can only deal with the single-objective alignment optimization problem and cannot optimize different objectives separately.

In summary, the limitations of existing studies on alignment optimization can be described as follows:

(1) From the aspect of problem modeling, most existing studies only consider a single-objective, e.g., costs, but neglect the environmental impacts of the railway or highway. In a few studies which consider an environmental objective, the environmental impacts are measured as the total area of the affected environmentally-sensitive region. However, it is hard to demarcate the environmentally-sensitive regions reasonably. The sensitivity of the environment to railway or highway construction in different regions also varies dramatically. Therefore, the environmental impacts cannot be measured accurately.

(2) From the aspect of solution method, most existing methods cannot optimize different objectives separately in a continuous space covering the entire study area.

To deal with limitation (1), new quantitative indexes for accurately measuring the environmental impacts are studied. The details of the new proposed indexes are provided in Section 3. To deal with limitation (2), we develop a multi-objective optimization method which can search for the alignment in continuous space and trade off different objectives effectively. The crucial problems and the solution methods are introduced in Section 4.

3. Problem specification

3.1. Design variables

An alignment can be determined by a set of points of intersection (PIs) between the endpoints in each head [5]. Points of intersection include both "horizontal points of intersection (HPIs)

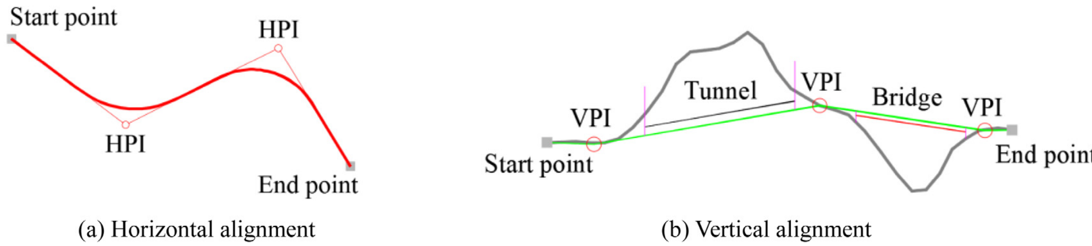

Fig. 1. A railway alignment.

and vertical points of intersection (VPIs) [18]". After the PIs are determined, they are connected with straight lines (called "tangents"). Then, a three-dimensional alignment can be generated by configuring curves at each PI to connect the tangents (Fig. 1) while satisfying all constraints.

Therefore, the specifications of HPIs and VPIs can be set as the design variables. Conventionally, the HPIs' specifications include the coordinates X_i, Y_i, horizontal curve radius R_i, and transition curve length l_{Ti}. The VPIs' specifications include the station K_i, design elevation H_i and vertical radius R_{Vi}. However, since l_{Ti} affects the alignment location and objective function value very slightly, and since the value of R_{Vi} is determined according to the railway grade in China, l_{Ti} and R_{Vi} are not included among the design variables [18]. Therefore, the basic alignment optimization problem is reduced to finding the vector sets of $\boldsymbol{X}$, $\boldsymbol{Y}$, $\boldsymbol{R}$, $\boldsymbol{K}$, $\boldsymbol{H}$.

$$\begin{aligned}
\boldsymbol{X} &= [X_1, X_2, \ldots, X_i, \ldots, X_m]^{\mathrm{T}} \\
\boldsymbol{Y} &= [Y_1, Y_2, \ldots, Y_i, \ldots, Y_m]^{\mathrm{T}} \\
\boldsymbol{R} &= [R_1, R_2, \ldots, R_i, \ldots, R_m]^{\mathrm{T}} \\
\boldsymbol{K} &= [K_1, K_2, \ldots, K_j, \ldots, K_n]^{\mathrm{T}} \\
\boldsymbol{H} &= [H_1, H_2, \ldots, H_j, \ldots, H_n]^{\mathrm{T}}
\end{aligned} \tag{1}$$

where "m is the number of HPIs, X_i and Y_i are the coordinates of the ith HPI, R_i is the horizontal curve radius of the ith HPI, n is the number of VPIs, K_j is the station of the jth VPI, and H_j is the design elevation of the jth VPI [18]".

For the railway alignment design problem, it is anticipated that the optimal alignment would largely follow the topographic contours or follow the lower-lying and relatively flatter terrain to reduce the construction cost. However, in environmentally-sensitive regions with fragile ecosystems and lush vegetation, the anticipated optimal alignment may have great negative impacts on the environment, such as vegetation destruction and soil erosion. Therefore, to optimize an alignment, designers should consider the costs and environmental impacts simultaneously.

3.2. Vegetation destruction evaluation

According to the Code for environmental protection design in railway engineering [29], railway alignment should pass through barren land as much as possible to prevent wholesale destruction of vegetation. As a railway alignment will traverse different regions, the vegetation growth status and vegetation coverage of the traversed regions will be different. To evaluate the damage to the vegetation, existing methods [23,24] usually demarcate some environmentally-sensitive regions before designing the alignment. Then, during the alignment optimization process, the total area of these regions traversed by the alignment is calculated. Finally, the calculated area is used as the quantitative index to evaluate the damage to the vegetation due to the railway construction. However, in mountainous regions with lush vegetation, it is hard to demarcate the environmentally-sensitive regions reasonably. The sensitivity of the environment to railway construction in different regions also varies dramatically. Therefore, the environmental impacts cannot be measured accurately.

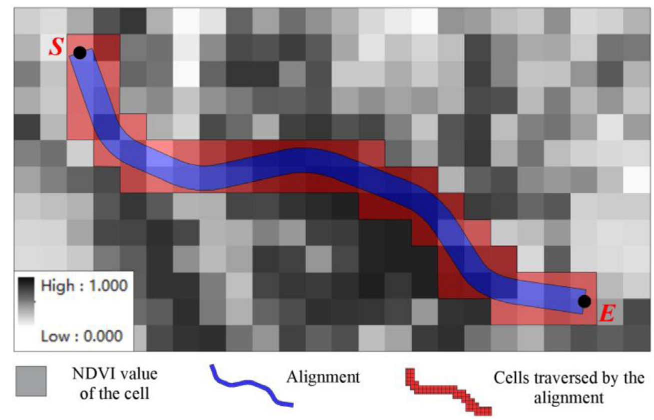

Fig. 2. Quantitative evaluation index of vegetation destruction.

In this study, we introduce the Normalized Difference Vegetation Index (NDVI) to evaluate the damage to vegetation due to the railway construction. NDVI is the most popular vegetation index which can reflect the vegetation growth status and vegetation coverage of a region [30]. This index is calculated with Eq. (2) and defines values from −1.0 to 1.0, where negative values are mainly due to clouds, water, and snow. Values close to zero are primarily due to rocks and bare soil, while values close to 1 reflect dense vegetation:

$$NDVI = \frac{\rho_{NIR} - \rho_{RED}}{\rho_{NIR} + \rho_{RED}} \tag{2}$$

where ρ_{RED} is radiance (in reflectance units) of a red channel near 0.66 μm, and ρ_{NIR} is radiance (in reflectance units) of a near-IR (infrared radiation) channel around 0.86 μm [31].

The latest NDVI data can be acquired from global datasets, such as SPOT (Satellite Pour l'Observation de la Terre) and MODIS (Moderate-Resolution Imaging Spectroradiometer), which can reflect the recent vegetation condition. We store the acquired NDVI data in the Comprehensive Geographic Information Model (CGIM) [2]. CGIM is a grid model which stores all the needed data for railway alignment optimization, such as topography, ground objectives, unit costs, coordinates of two endpoints, forbidden zones, railway major technical standards, and code provision parameters. We sum the positive NDVI values of all the cells through which the alignment passes and set the overall NDVI value as the quantitative evaluation index (as shown in Fig. 2). Then, the damage to vegetation can be accurately evaluated based on the recent vegetation condition.

The overall NDVI value is calculated with Eq. (3):

$$SV_{NDVI} = \sum_{\forall C^{(k)} \in \mathbf{U_S}} \max\left\{V_{NDVI}^{(k)}, 0\right\} \tag{3}$$

where SV_{NDVI} is the overall NDVI value, $C^{(k)}$ is the kth cell traversed by the alignment, $\mathbf{U_S}$ is the set of cells traversed in the form of the fill or cut sections, and $V_{NDVI}^{(k)}$ is the NDVI value of the

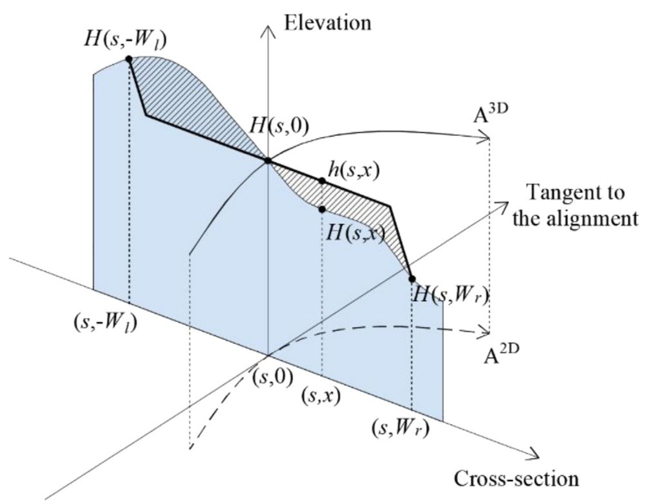

Fig. 3. Cross section at the mileage of s.

kth cell. It should be noted that only the cells which the alignment traverses in the form of fill or cut sections (i.e. excluding bridges and tunnels) are considered in the calculation.

3.3. Soil erosion evaluation

Soil erosion is a major environmental threat to the "sustainability and productive capacity of agriculture [32]". According to the Code for environmental protection design of railway engineering [29], the soil erosion caused by railway construction should be minimized to conserve the soil and water. Since spoil is the major cause of soil erosion [33], we use the spoil volume as the quantitative index to evaluate the level of soil erosion caused by railway construction. The spoil volume is used here as a proxy variable for soil erosion. The total spoil volume (V_S) is calculated with Eq. (4) according to the volume of cut sections (V_{SC}), the cut volume of tunnels (V_{TC}), and the volume of fill sections (V_{SF}).

$$V_S = \max\{V_{SC} + V_{TC} - V_{SF}, 0\} \tag{4}$$

The volumes of cut sections V_{SC} and fill sections V_{SF} are calculated with Eqs. (5) and (6), respectively, as shown in Fig. 3 [34], where A^{3D} represents the 3-dimension alignment, A^{2D} represents the projection of the alignment on the 2-dimension plane (i.e., the horizontal alignment):

$$V_{SC} = \int_0^L \int_{-W_l}^{W_r} \max\{H(s,x) - h(s,x)\ , 0\}\, dxds \tag{5}$$

$$V_{SF} = \int_0^L \int_{-W_l}^{W_r} \max\{h(s,x) - H(s,x)\,, 0\}\, dxds \tag{6}$$

where L is the total length of the alignment, W_l and W_r are the widths of the left and right sides of the subgrade, s represents the distance along the alignment, $s \in [0, L]$. Function $H(.)$ specifies the terrain elevation, and function $h(.)$ provides the design elevation.

The cut volume of tunnels (V_{TC}) is calculated with Eq. (7):

$$V_{TC} = \sum_{i=1}^{n} \int_{T_S^{(i)}}^{T_E^{(i)}} AT^{(i)} ds \tag{7}$$

where n is the number of tunnels, $T_S^{(i)}$ and $T_E^{(i)}$ are the start and end stations of the ith tunnel, and $AT^{(i)}$ is the cross section area of the ith tunnel.

3.4. Economic evaluation

Cost is usually the most important factor affecting railway alignment design. In the existing literature on alignment optimization, various economic objective functions including construction cost (C_C) and operating cost (C_O) have been formulated [1,5,16,28]. In this study, the objective functions from our previous study [2] are used. These are specified as:

$$C_C = \Delta\cdot(C_B+C_T+C_E+C_L+C_R) \tag{8}$$

$$C_O = C_A + C_M+C_G \tag{9}$$

where "Δ is the capital recovery factor. It is usually set at 0.065 in China [2]". C_B, C_T, and C_E are the construction costs of bridge, tunnel, and earthwork, C_L and C_R are the length-dependent cost and right-of-way cost, C_A, C_M, and C_G are the operating costs which are sensitive to HPI deflection angle, alignment length, and vertical gradient. Detailed formulations of the objective functions are provided in our previous publication [2].

3.5. Constraints

One important constraint for the alignment optimization problem is to bypass forbidden zones in an environmentally-sensitive area. The regions of nature reserve, wildlife habitats isolation, and water source protection are usually defined as forbidden zones which the alignment must bypass.

Besides the forbidden zone constraints, there are also many other constraints, such as the minimum radius of the horizontal circular curves (R_{min}), the maximum gradient of vertical slope sections (G_{max}), and the crossing constraints [35]. Li et al. [18,36] classify these multiple constraints into "geometric constraints, location constraints, construction constraints and denote them as $g_i(\boldsymbol{X,Y,R,K,H})\leq 0$, $l_i(\boldsymbol{X}, \boldsymbol{Y,R,K,H})$, $c_i(\boldsymbol{X,Y,R,K,H})\leq 0$", respectively. Detailed specifications of these constraints are provided in Li et al. [18].

3.6. Model formulation

The multi-objective railway alignment optimization model is formulated as follows:
Objective:
O1: Minimize the overall NDVI value of the cells traversed by the alignment.

$$Min\, f_{SV_{NDVI}}(\boldsymbol{X}, \boldsymbol{Y}, \boldsymbol{R}, \boldsymbol{K}, \boldsymbol{H}) = \sum_{k=1}^{n_c} V_{NDVI}^{(k)} \tag{10}$$

O2: Minimize the total spoil volume.

$$Min\, f_{V_S}(\boldsymbol{X}, \boldsymbol{Y}, \boldsymbol{R}, \boldsymbol{K}, \boldsymbol{H}) = \max\{V_{SC} + V_{TC} - V_{SF}, 0\} \tag{11}$$

O3: Minimize the total costs ($C_C + C_O$).

$$Min\, f_{T-investment}(\boldsymbol{X}, \boldsymbol{Y}, \boldsymbol{R}, \boldsymbol{K}, \boldsymbol{H}) = \Delta(C_B + C_T + C_E + C_C + C_R) + C_A + C_M + C_G \tag{12}$$

Constraints:
C.t.1: Geometric constraints $g_i(\boldsymbol{X,Y,R,K,H})\leq 0$.
C.t.2: Location constraints $l_i(\boldsymbol{X}, \boldsymbol{Y,R,K,H})\leq 0$.
C.t.3: Construction constraints $c_i(\boldsymbol{X,Y,R,K,H})\leq 0$.

4. The proposed PSO-based multi-objective optimization method

The multi-objective model formulated in this study is solved with a PSO-based multi-objective optimization method. New update mechanisms are proposed for dealing with the multi-objective optimization problem and a local repair algorithm is designed for the alignment design problem. The procedure of the proposed method is shown in Fig. 4.

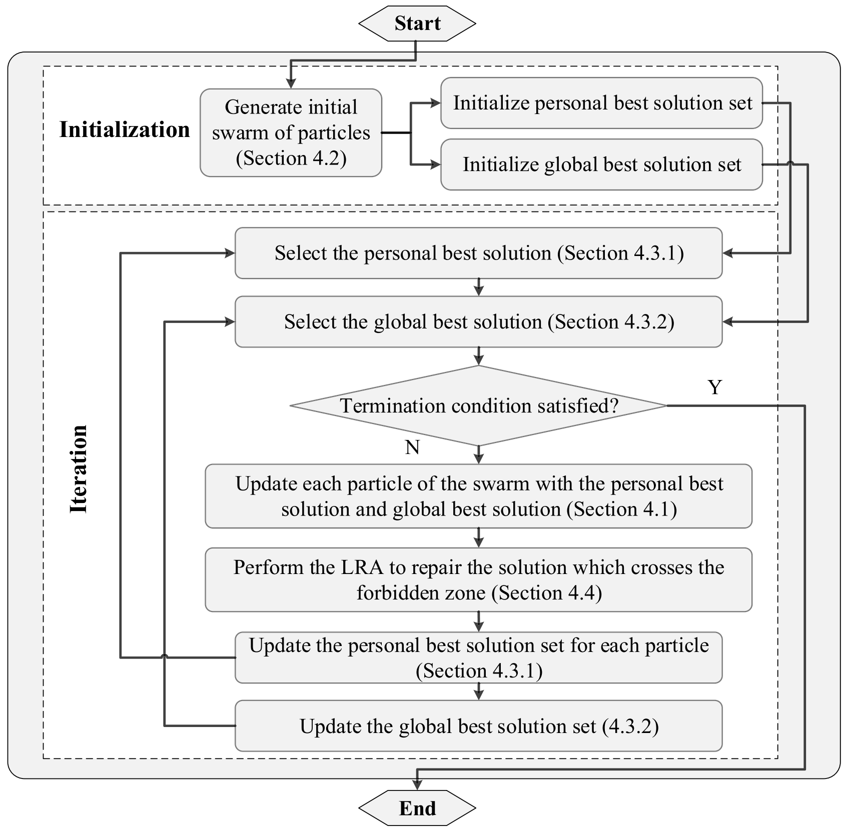

Fig. 4. Procedure of the proposed method.

4.1. The basic PSO algorithm

The PSO algorithm usually starts with a population of particles. The potential solutions of the studied problem are represented by the positions of these particles. The position of each particle is determined according to the design variables of the studied problem. These particles fly through the study area to find the optimal position. During this process, each particle is characterized by a fitness value and a velocity value [37]. The fitness value is calculated according to the objective function of the studied problem while the velocity is used to determine the flight direction and speed. In each iteration the velocity of each particle is updated according to the current velocity and two best positions, which are the personal best position (*pbest*) the global best position (*gbest*). *pbest* is the position of the particle which has the best fitness value obtained so far by itself and *gbest* is the position of the particle which has the best fitness value obtained so far by the entire swarm. The position of each particle is updated based on the current position and the updated velocity, as shown in Eqs. (13) and (14):

$$\boldsymbol{Vel_i}(t+1) = w \cdot \boldsymbol{Vel_i}(t) + C_1 \cdot r_1(t) \cdot [\boldsymbol{gbest}(t) - \boldsymbol{Pos_i}(t)] + C_2 \cdot r_2(t) \cdot [\boldsymbol{pbest}(t) - \boldsymbol{Pos_i}(t)] \tag{13}$$

$$\boldsymbol{Pos_i}(t+1) = \boldsymbol{Pos_i}(t) + \boldsymbol{Vel_i}(t+1) \tag{14}$$

where the lower foot label i denotes the ith particle in the swarm, t is the current iteration, C_1 and C_2 are acceleration coefficients, whose most frequent values are C_1=C_2=2 [38], r_1 and r_2 are random numbers that are uniformly distributed in the range [0,1], and w is the inertia weight proposed by Shi and Eberhart [39].

To illustrate these two equations, the updating process in a two-dimensional space is provided, as shown in Fig. 5.

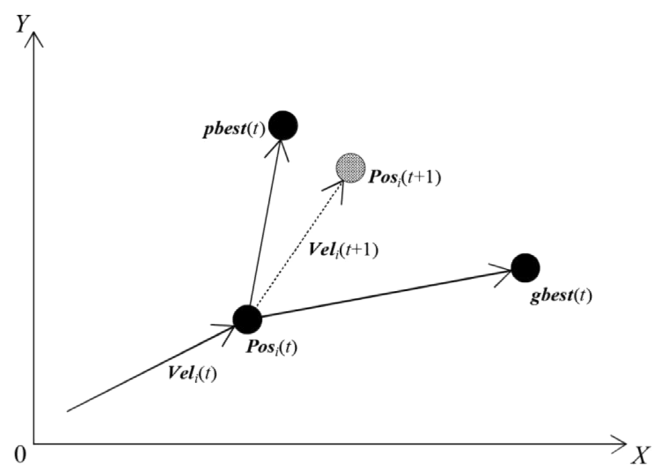

Fig. 5. The updating process of PSO in a two-dimensional space.

4.2. Initialization

Generating a set of high-quality solutions in the initialization can accelerate the convergence speed of the PSO algorithm [37]. For this purpose, the Distance Transform algorithm [2] is used to generate an optimized path (i.e., the black line in Fig. 6). Then, a set of butterfly-shaped areas [3] and angular bisectors is generated according to each key point of the path. The offsets (i.e., L1, L2, and L3 in Fig. 6) and deflections (i.e., $\alpha 1$, $\alpha 2$, and $\alpha 3$ in Fig. 6) of initial HPIs to key points are randomly generated. The coordinates of the initial HPIs are calculated according to their offsets and deflections. The initial horizontal alignment (i.e., the purple line in Fig. 6) is generated by configuring curves at each HPI. To initialize the VPIs, a set of orthonormal cutting planes

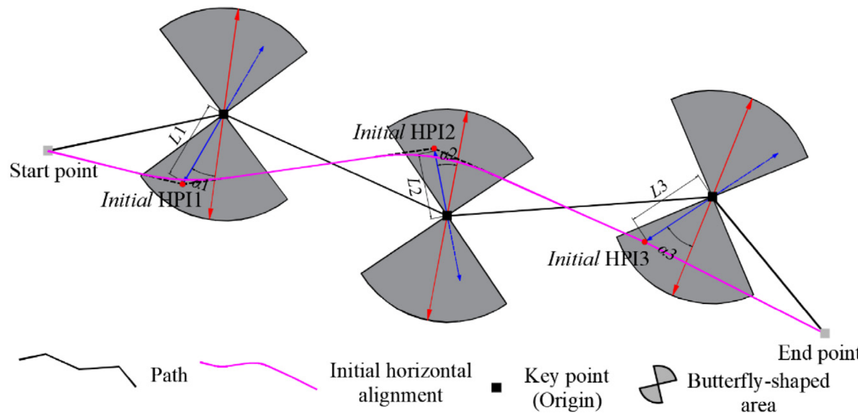

Fig. 6. Initialization of horizontal alignment.

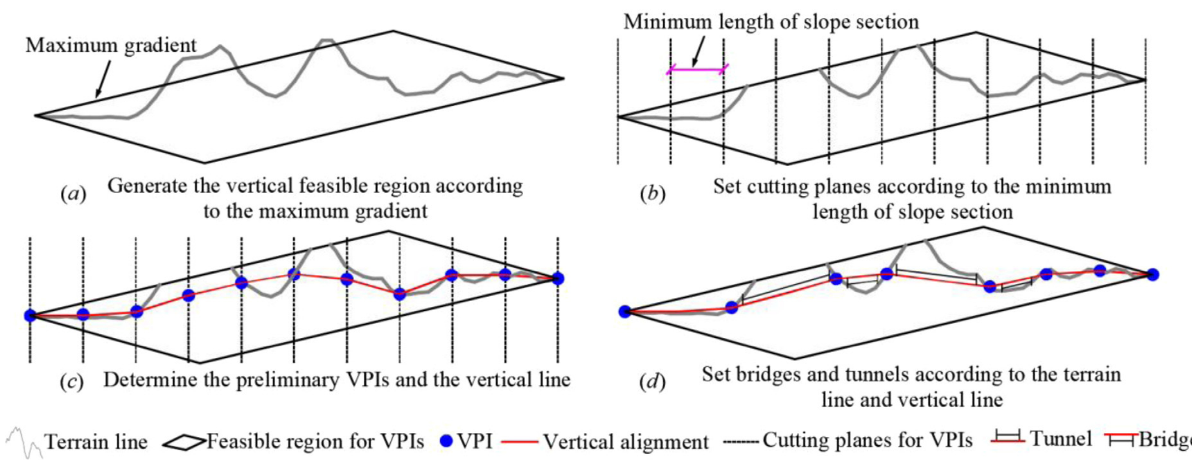

Fig. 7. Initialization of vertical alignment.

along the horizontal alignment is generated according to the minimum length of gradient section and the maximum gradient [40]. The initial VPIs are randomly distributed on each cutting plane within the feasible region, which is determined according to the maximum gradient, as shown in Fig. 7. The detailed initialization process can be found in the authors' earlier publication [3].

4.3. Mechanisms of multi-objective optimization

A fundamental task of the PSO algorithm is to find the *pbest* and *gbest* solutions. For the single-objective optimization problems, the *pbest* and *gbest* solutions can be determined according to the fitness value.

However, in the multi-objective railway alignment optimization problem, it is usually impossible to find just one solution which can dominate all others. Instead, a number of non-dominated solutions are usually found. For multi-objective optimization problems, a solution s_i is said to dominate another solution s_j if and only if there is at least one objective function value of s_i is better than the corresponding objective function value of s_j and the remaining objective function values of s_i are not worse than the corresponding objective function values of s_j. When a solution is not dominated by any other solution, it is called a non-dominated solution or a Pareto-optimal solution.

Therefore, determining the *pbest* and *gbest* solutions in each iteration is a crucial problem. To solve it, two new mechanisms are designed for identifying and updating the *pbest* and *gbest* solutions.

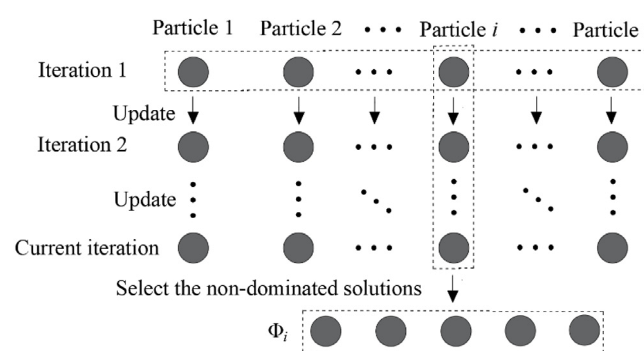

Fig. 8. Personal best solution set Φ_i.

4.3.1. pbest solution determining mechanism

In this study, each particle i is allowed to have an archive that stores the non-dominated solutions it has obtained so far, which form a personal best solution set $\boldsymbol{\Phi_i}$. Fig. 8 provides an illustration, where the circles represent all the solutions (i.e., positions of the particles) which are generated until the current iteration. The maximum size of $\boldsymbol{\Phi_i}$ is set as n_p. When the size of $\boldsymbol{\Phi_i}$ exceeds n_p, the solutions which rank after n_pth are discarded. The sensitivity analysis of n_p for a real-world case is provided in Section 5.1.2.

To rank the non-dominated solutions in each personal best solution set $\boldsymbol{\Phi_i}$, the multi-criteria tournament decision (MTD) method is introduced. MTD [41], first proposed by Parreiras and Vasconcelos, is a multi-criteria analysis method, which can rank non-dominated solutions according to the preferences of the human decision-maker. There are two important functions of the MTD method, namely the tournament function $T^{(j)}(a, \Phi_i)$ (Eq. (15)) and the ranking function $R(a)$ (Eq. (18)). The tournament function $T^{(j)}(a, \Phi_i)$ is used to implement the pairwise comparison of all the solutions in $\boldsymbol{\Phi_i}$ and counts the ratio of times the solution a wins the tournament against every other b solution on the jth objective, as shown in Eq. (15).

$$T^{(j)}(a, \boldsymbol{\Phi}_i) = \sum_{\forall b \in \Phi_i \wedge a \neq b} \frac{t^{(j)}(a, b)}{(|\boldsymbol{\Phi}_i| - 1)} \tag{15}$$

For the alignment optimization problem in this study, the winner of each tournament is the solution with the lower objective function value. Therefore, in Eq. (15), $t^{(j)}(a, b)$ is defined as:

$$t^{(j)}(a, b) = \begin{cases} 1, \text{ if } f^{(j)}(a) < f^{(j)}(b) \\ 0, \text{ if } f^{(j)}(a) \geq f^{(j)}(b) \end{cases} \tag{16}$$

where $f^{(j)}(a)$ and $f^{(j)}(b)$ are the values of the jth objective function of solutions a and b.

Each solution in $\boldsymbol{\Phi_i}$ is assigned a set of winning ratios by the tournament function $T^{(j)}(a, \Phi_i)$. Based on the winning ratios, the ranking function $R(a)$ is implemented to calculate the solution's ranking index. The weighted geometric mean given in Eq. (17) is one of the widely used ranking functions [41].

$$R(a) = \left(\prod_{j=1}^{m} T^{(j)}(a, \boldsymbol{\Phi}_i)^{w_j} \right)^{1/m} \tag{17}$$

By using this ranking function, the ranking index of the *ith* solution is 0 if the winning ratio of one objective of this solution is 0. If we just want to find the comprehensive optimal solution from a set of Pareto-optimal solutions, the weighted geometric mean is effective. The solution would not be useful if it performs very poorly in one objective.

However, in this study, the ranking function should have the ability to find the best solution to improve the performance of the swarm in each iteration during the optimization process. For the alignment optimization problem, there may exist such situations in which a solution performs better than the other solutions in all objectives except for one. In such situations, the ranking index is 0 if the weighted geometric mean is used. However, in this study, this solution still has value, especially when the weight of the poorly performing objective is very low. Therefore, the ranking index of the solution in this situation should not be 0. To solve this problem, a new ranking function is proposed in this study, as shown in Eq. (18):

$$R(a) = \sum_{j=1}^{m} w_j \cdot T^{(j)}(a, \boldsymbol{\Phi}_i) \tag{18}$$

where w_j is the weight of the jth objective and m is the number of objective functions (which is 3 in the alignment optimization problem of this study).

By using this ranking function, the ranking index of the solution will not be 0 when the situation mentioned above occurs and it can also reflect the comprehensive performance of the solution considering the objective weights.

The ranking index is used as the fitness value and the non-dominated solutions in Φ_i are sorted according to the ranking index. Finally, the highest ranked solution is selected as the personal best solution and used to update the velocity of particle i with Eq. (13).

4.3.2. gbest solution determining mechanism

A good multi-objective evolutionary algorithm should obtain solutions with (a) good convergence as well as (b) good diversity and spread along the Pareto-optimal front [42]. Unlike determining the personal best solution which is mainly used to guarantee the convergence of the solutions, determining the global best solution should also guarantee the diversity of the solutions. To solve this problem, Zhang et al. [37] proposed a mechanism to determine the global best solution based on the crowding value. In their study, a solution with lower crowding value was given priority. The present study improved Zhang et al.'s mechanism, which determines the global best solution according to both the objective function values and the crowding value. The mechanism is described as follows.

First, an external archive is employed. The non-dominated solutions of the entire swarm are stored in the archive forming the global best solution set Φ. The number of solutions in Φ cannot exceed a given parameter n_g. We provide a sensitivity analysis of n_g for a real-world case in Section 5.1.2.

Then the crowding value (ρ_a) of each solution in Φ is calculated. We rank the solutions according to the crowding values. A solution with a lower crowding value is ranked higher and only the first n_g solutions are kept. (See the Crowding value calculation process.)

After obtaining the crowding-based ranking list which is named **R1**, we also rank the solutions in Φ using the MTD method in Section 4.3.1 and obtain another ranking list named **R2**. Finally, the *gbest* solution is determined according to both **R1** and **R2** using the roulette wheel selection method [43]. Assuming solution s_i in Φ is ranked as $R1_{si}$ and $R2_{si}$ under the two ranking lists, the probability of selecting solution s_i (P_{si}) is assigned with Eq. (19).

$$P_{si} = \frac{2(|\boldsymbol{\Phi}| + 1) - R1_{si} - R2_{si}}{|\boldsymbol{\Phi}|(|\boldsymbol{\Phi}| + 1)} \tag{19}$$

Table 1
Probability of selecting each solution.

Solution no.	R1	R2	Probability
Solution 1	1	2	7/20
Solution 2	2	3	5/20
Solution 3	3	1	6/20
Solution 4	4	4	2/20

For example, if Φ contains four solutions whose ranking lists are shown in Table 1, the probability of selecting each solution in Φ is 7/20, 5/20, 6/20, and 2/20, respectively.

It should be noted that, in this study, we mainly focus on solving the crowding problem in objective space. The problem of crowding in design space is considered in our previous work [3]. A stepwise & hybrid particle swarm-genetic algorithm, which is the basis of this study, is developed to solve the problem. The detailed algorithm can be found in Pu et al. [3].

4.4. The local repair algorithm (LRA)

For the railway alignment optimization problem, the final alignment must bypass the pre-specified forbidden zones (e.g., nature reserve, wildlife habitats isolation). In existing methods, to ensure that forbidden zones are bypassed, any alignment which crosses the forbidden zones is discarded. However, in an environmentally-sensitive area with many forbidden zones, such methods may miss many valuable solutions during the search process, thereby limiting the quality of the final optimized alignment. Therefore, to solve this problem, a local repair algorithm (LRA) is proposed based on a customized crossover operator.

The LRA module is embedded in the framework of the proposed method (Fig. 4) and operates in each iteration. As soon as all the solutions in the entire swarm of particles are updated, the

Crowding value calculation process	
for each $a \in \boldsymbol{\Phi}$, set $\rho_a = 0$	initialize crowding value of each solution in Φ
for each $a \in \boldsymbol{\Phi}$ for each $b \in \boldsymbol{\Phi}$, $b \neq a$ $D(a, b) = \sqrt{\sum_{j=1}^{m} \left(\frac{f^{(j)}(a) - f^{(j)}(b)}{f^{(j)}_{\max}(\boldsymbol{\Phi}) - f^{(j)}_{\min}(\boldsymbol{\Phi})} \right)^2}$	calculate the distance between every pair of solutions
for each $a \in \boldsymbol{\Phi}$ *sort* $[a, D(a, b)]$	Sort in ascending using the calculated distance (e.g., for the solution a, the first of the ranking is the solution that is closest to a)
$\rho_a = \frac{1}{\left((1/k) \sum_{r=1}^{k} D_a^{(r)} \right)}$	calculate the crowding value

* m is the number of objective functions (which is 3 in the present alignment optimization problem).
* $f^{(j)}_{\max}(\boldsymbol{\Phi})$ and $f^{(j)}_{\min}(\boldsymbol{\Phi})$ are the maximum and minimum values of the jth objective function among the solutions in $\boldsymbol{\Phi}$.
* k is used to rule only the first kth solutions in Φ are used to calculate the crowding value of each solution.
* $D_a^{(r)}$ denotes the distance between a and the solution that is the rth closest to a (i.e., $r = 1, \ldots, k$).

LRA is performed. The solutions which cross the forbidden zones are replaced with the repaired solutions produced by the LRA and the new swarm undergoes the *pbest* and *gbest* determining procedures as described in Section 4.3. A detailed description of the LRA is provided below.

4.4.1. The customized crossover operator

Crossover operators, such as simple crossover, two-point crossover, arithmetic crossover, and heuristic crossover, are widely used in genetic algorithms (GAs). Normally, these crossover operators operate between two solutions and the crossing positions are random. The newly generated solutions through these crossover operators may be better or worse than the original solutions. The main function of these crossover operators in GA is to increase the population diversity, in order to find better solutions.

However, in this subsection, our purpose is to develop an operator which can efficiently repair solutions that cross the forbidden zones. Therefore, a customized crossover operator is proposed. The crossing section is predetermined before performing the crossover operator. We directly replace the HPIs of the section which crosses the forbidden zones with the corresponding HPIs of the nearest sections. The implementation details of the customized crossover operator are described in Section 4.4.2.

4.4.2. An illustrative example

To illustrate how the local repair algorithm works, an artificial example is designed. This example has one forbidden zone and three alignments, as shown in Fig. 9. The red alignment crosses the forbidden zone and the other two alignments bypass the forbidden zone. The repair procedure for this alignment is described below.

[Step 1] Check along the red alignment and select the section which crosses the forbidden zone. The selected section is between the 2nd and 4th HPIs (Fig. 9*a*).

[Step 2] Calculate the distance between the selected section of the red alignment and the corresponding sections of the blue alignment (D_{r-b}) and the yellow alignment (D_{r-y}) with Eq.s (20) and (21):

$$D_{r-b} = \sum_{i=3,4,5} \sqrt{\left(x^{(i)}_{red} - x^{(i)}_{blue}\right)^2 + \left(y^{(i)}_{blue} - y^{(i)}_{blue}\right)^2} \tag{20}$$

$$D_{r-y} = \sum_{i=3,4,5} \sqrt{\left(x^{(i)}_{red} - x^{(i)}_{yellow}\right)^2 + \left(y^{(i)}_{red} - y^{(i)}_{yellow}\right)^2} \tag{21}$$

where $(x^{(i)}_{red}, y^{(i)}_{red})$, $(x^{(i)}_{blue}, y^{(i)}_{blue})$, and $(x^{(i)}_{yellow}, y^{(i)}_{yellow})$ are the coordinates of the ith HPI of the red, blue, and yellow alignment, respectively. The nearest one (i.e., the corresponding section of the blue alignment, as shown in Fig. 9*b*) is chosen for the next step.

[Step 3] Replace the HPIs of the selected section of the red alignment with the HPIs of the corresponding section of the blue alignment and generate the repaired alignment (Fig. 9c).

5. Case study

This method has been employed by China Railway Eryuan Engineering Group CO. LTD and applied to many real-world railway alignment design projects, such as Sichuan–Tibet, Chengdu–Lanzhou, and China–Pakistan. In this section, two railway cases are presented to demonstrate the effectiveness of the proposed method. The first railway case is from Songzong to Bomi, which is a section of Sichuan–Tibet Railway. Through this railway case, the sensitivities of two specific parameters (i.e., n_p, n_g) of the developed method in this study are analyzed and the effectiveness of the method is verified by setting different objective weights. The second railway case is from Maoxian to Taiping, which is a section of the Chengdu–Lanzhou railway. This railway case is larger than the first one and we compare the developed method in this study with the method developed in our previous work [3].

5.1. The first railway case

5.1.1. Railway case profile

The Songzong–Bomi Railway is a Grade I railway, which passes through an environmentally-sensitive region with fragile ecosystems and lush vegetation. The coordinates (in the 3-D Cartesian coordinate system) of the start and end points are S (3292099.157, 32510156.707, 3034.906) and E (3304500.333, 32476982.557, 2730.593), respectively. The airline distance between the start and end points is 35416.287 m. The size of the study area is 836 sq. kilometers (38 km × 22 km). It is represented with 836 rectangular lattice cells (30 m × 30 m). The topography of the study area is shown in Fig. 10 and the corresponding NDVI diagram is shown in Fig. 11. The symbols "S" and "E" in these figures represent the start and end points of the alignment, respectively. From the NDVI diagram, we can see the NDVI value in more than half the area is nearly 1 (i.e., red area), which indicates very dense vegetation in the study area. The topography data used in this

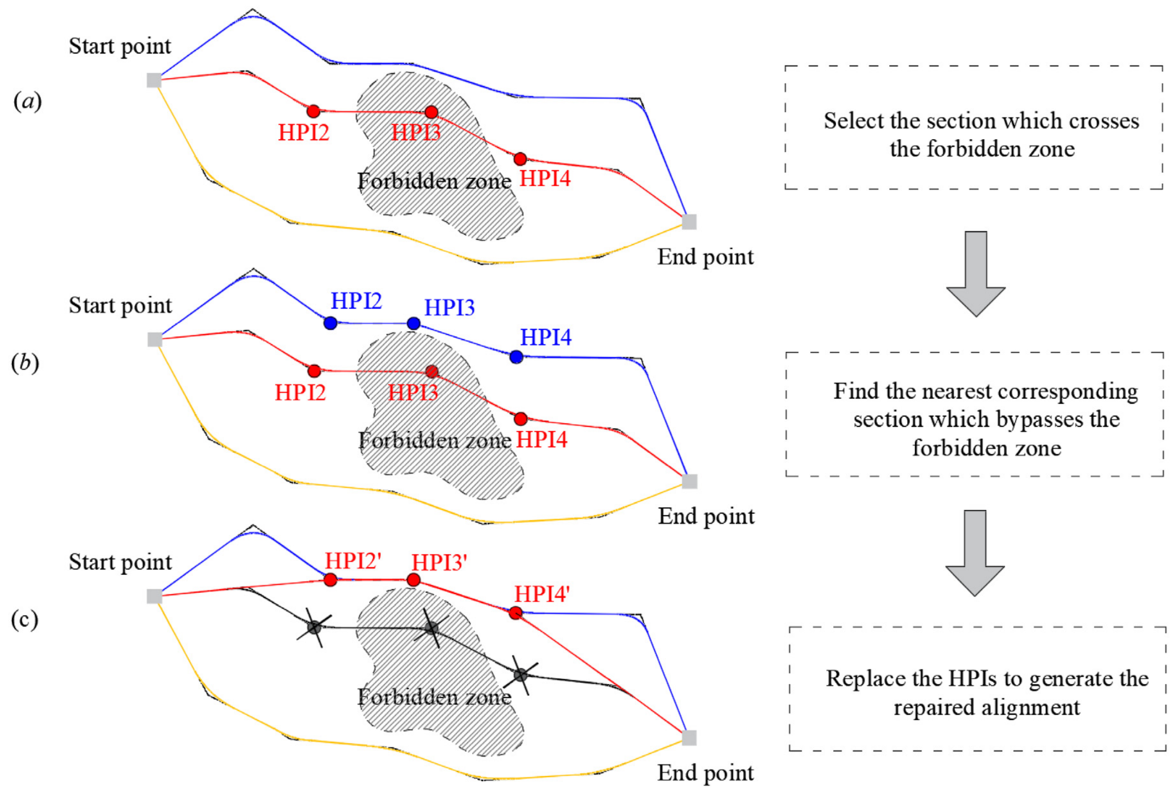

Fig. 9. An example of the repair process using the LRA.

Table 2
Unit costs.

Item	Cost	Item	Cost
Rail track (¥/m)	4000	Filling earthwork (¥/m^3)	18
Right-of-way (¥/m^2)	90	Cutting earthwork (¥/m^3)	20
($L\geq$1000 m) Tunnel (¥/m)	60,000	(H<50) Bridge (¥/m)	37,800
($L\geq$400 m) Tunnel (¥/m)	56,000	($H\geq$50, L<500 m) Bridge (¥/m)	48,800
(L<400 m) Tunnel (¥/m)	54,000	($H\geq$50, $L\geq$500 m) Bridge (¥/m)	58,800
One tunnel portal (¥)	250,000	One abutment (¥)	200,000
Capital recovery factor Δ	0.065		

case are downloaded from the Geospatial Data Cloud website (http://www.gscloud.cn), whose resolution is 30 m. The NDVI data used in this case are downloaded from the Resource and Environment Data Cloud Platform (http://www.resdc.cn), whose resolution is 1 km.

5.1.2. Parameter setting

For this case, the key input parameters (i.e., unit costs, railway major technical parameters, constraints, and PSO parameters) are set according to the information provided by the China Railway Eryuan Engineering Group Co. Ltd, the authors' earlier publications [3,18], and experiments discussed below.

The unit costs are the same as in Li et al. [18], as shown in Table 2. The railway's major technical parameters and considered constraints are provided by the China Railway Eryuan Engineering Group Co. Ltd, as listed in Tables 3 and 4.

The PSO parameters are set according to Pu et al. [3], who have analyzed the sensitivities of the railway alignment optimization problem to the swarm size, learning factors, and maximum velocity. As the terrain condition and airline distance of this railway case are similar to those of the railway case in Pu et al. [3], we determine the values for the swarm size, learning factors, and maximum velocity by referring to the results of Pu et al. [3]. However, in this study, there are another two key parameters for the multi-objective railway alignment optimization problem,

Table 3
Railway major technical parameters.

Major technical standards	Recommendation
Railway grade	Grade I
Design speed	200 km/h
Main line number	Double
Vertical circular curve radius	10000 m
Fill-bridge threshold height	10 m
Cut-tunnel threshold depth	−15 m

i.e., the maximum size of personal best solution set (n_p) and global best solution set (n_g). To determine the values of these two parameters, the design of experiments (DOE) method is applied and each parameter is tested at 4 different levels ($n_p \in \{24, 28, 32, 36\}$, $n_g \in \{60, 70, 80, 90\}$). A total of 16 scenarios with different combinations of n_p and n_g are examined, as shown in Table 5.

Since C-metric (CM) is the most relevant indicator of solution quality in the multi-objective optimization context [37], we introduce CM as the performance indicator to judge which scenario is better, as shown in Eq. (22):

$$C(s_1, s_2) = \frac{|\{\mathbf{x}_2 \in \mathbf{S}_2 : \exists \mathbf{x}_1 \in \mathbf{S}_1, \mathbf{x}_1 \preceq \mathbf{x}_2\}|}{|\mathbf{S}_2|} \tag{22}$$

where $\mathbf{S}_1$ and $\mathbf{S}_2$ are the solution sets of s_1 and s_2, respectively, $\mathbf{x}_1 \preceq \mathbf{x}_2$ indicates that solution $\mathbf{x}_1$ dominates or is identical to

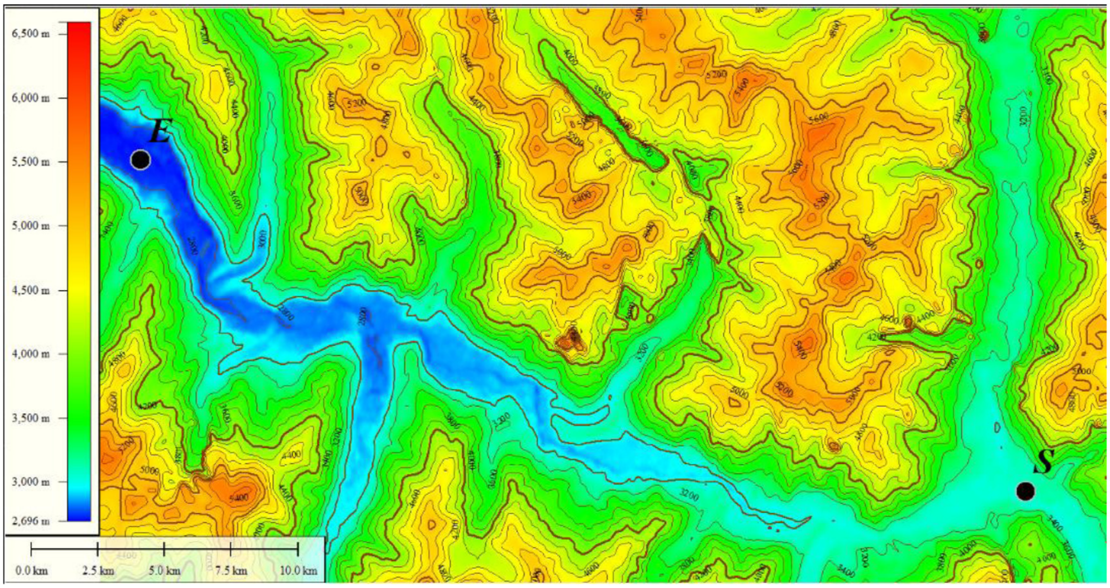

Fig. 10. Topography data in ASC format.

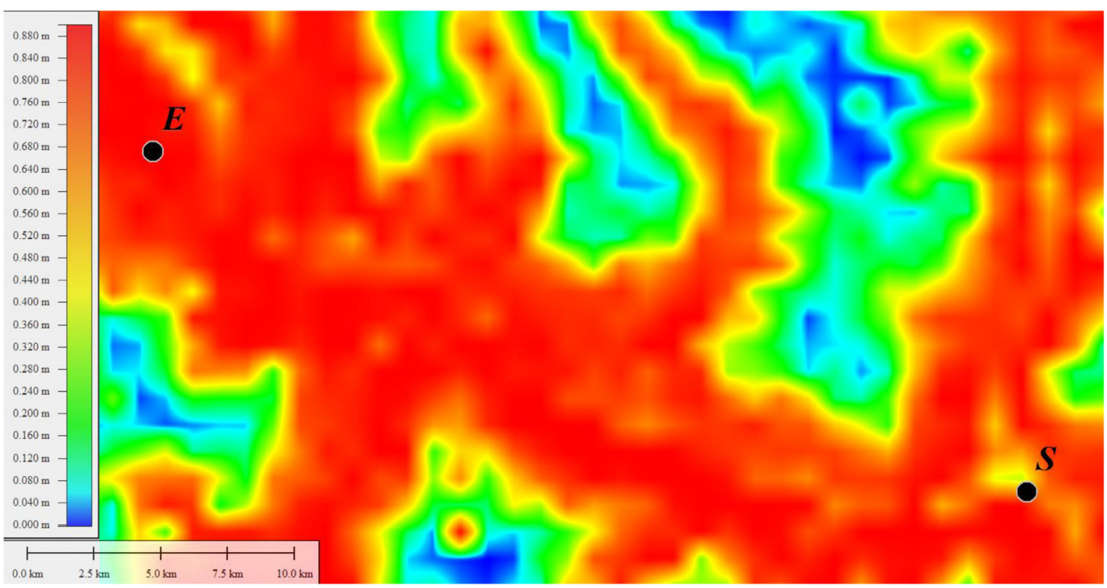

Fig. 11. NDVI data in ASC format.

Table 4
Main constraints.

Classes	Item	Value
Geometric constraints	Minimum radius of curve	2800 m
	Maximum gradient	24‰
	Minimum length of tangent between horizontal curves	120 m
	Minimum length of horizontal circular curve	120 m
	Minimum length of gradient section	250 m
	Absolute difference between adjacent gradients	18‰
Construction constraints	Maximum bridge height	100 m
	Maximum tunnel length	20,000 m
	Terminals are not overlapping with tunnels	
Location constraints	Bypass 6 forbidden zones	
	If crossing river, clearance $\geq$ 6 m	
	Elevation tendency: keep increasing alignment elevation	

$\mathbf{x}_2$, $C(s_1, s_2)$ indicates the ratio of the solutions in $\mathbf{S}_2$ that are dominated by (or identical to) the solutions in $\mathbf{S}_1$. If $C(s_1, s_2)$ is larger than $C(s_2, s_1)$ then s_1 is superior to s_2.

The CM value of each pair among the 16 scenarios is shown in Table 6.

According to Table 6, s_9, s_{10}, s_{11}, and s_{12} are superior to the other scenarios. The n_p values of these 4 scenarios are all 32

Table 5
n_p and n_g values of the 16 scenarios.

n_p	n_g			
	60	70	80	90
24	s_1 (24,60)	s_2 (24,70)	s_3 (24,80)	s_4 (24,90)
28	s_5 (28,60)	s_6 (28,70)	s_7 (28,80)	s_8 (28,90)
32	s_9 (32,60)	s_{10} (32,70)	s_{11} (32,80)	s_{12} (32,90)
36	s_{13} (36,60)	s_{14} (36,70)	s_{15} (36,80)	s_{16} (36,90)

and the value of n_g does not affect the final solution set when the n_g value exceeds 70. Therefore, the values of n_p and n_g are determined as 32 and 70, respectively. All the PSO parameters used for this case are shown in Table 7.

5.1.3. Experiment design

For this case, the following three objectives are optimized:

Objective 1: Minimize the vegetation destruction in the railway construction with Eq. (10).

Objective 2: Minimize the soil erosion caused by the railway construction with Eq. (11).

Objective 3: Minimize the total costs of the railway with Eq. (12).

Four scenarios with different objective weights are tested for the railway case. The assumed objective weights are listed in Table 8. The program runs on the HP Z600 workstation (Intel Xeon E5506 2.13 G processor, 4 GB RAM, 500 GB Hard disk).

5.1.4. Experimental results and analyses

The total elapsed times of Scenarios 1, 2, 3, and 4 are 29.552 min, 33.168 min, 36.465 min, and 70.183 min, respectively. To normalize the values of the three objectives, the Min–max normalization method is used, as defined in Eq. (23):

$$y_i = \frac{x_i - \min x_i}{\max x_i - \min x_i} \tag{23}$$

where x_i is the value of the ith objective and y_i is the corresponding normalized value, min x_i is the minimum value of the ith objective among all the non-dominated solutions, and max x_i is the maximum value of the ith objective among all the non-dominated solutions.

To compare the obtained non-dominated solutions of the four scenarios, we combine the non-dominated solutions obtained in Scenario 4 with the non-dominated solutions obtained in the other three scenarios and normalize the objective values based on the maximum and minimum values of the combined solution set. Based on the normalized objective values, the obtained Pareto-optimal Fronts in Scenario 4 and the other three scenarios are compared in Fig. 12.

As shown in Fig. 12, the non-dominated solutions obtained in Scenario 4 are more evenly distributed. The results of the other three scenarios are more concentrated around the area where the value of the highly weighted objective is low. Furthermore, in the direction of the highly weighted objective, the non-dominated solutions of Scenarios 1, 2, and 3 lie on a layer outside that of the non-dominated solutions of Scenario 4, which implies that the obtained Pareto-optimal Front is closer to the true Pareto-optimal Front in the direction of the highly weighted objective. These results demonstrate that the proposed method can consider the weights of different objectives and trade off objectives during the optimization process.

To further compare the non-dominated solutions of the four scenarios, we select the best solution of each scenario according to the preference information, using Eq. (24):

$$CV'^{(j)} = w_1 \cdot (C_C'^{(j)} + C_O'^{(j)}) + w_2 \cdot SV_{NDVI}'^{(j)} + w_3 \cdot V_S'^{(j)} \tag{24}$$

where $C_C'^{(j)}$ and $C_O'^{(j)}$ are the normalized construction and operating costs of the jth non-dominated solution, $SV_{NDVI}'^{(j)}$ is the normalized overall NDVI value of the jth non-dominated solution, $V_S'^{(j)}$ is the normalized spoil volume of the jth non-dominated solution, and w_1, w_2, w_3 are the weights of the three objectives, as shown in Table 8.

The selected best solutions are termed as Alt1, Alt2, Alt3, and Alt4. The horizontal and vertical alignments of these four solutions are shown in Fig. 13. The detailed results are presented in Table 9.

Table 7
PSO parameters.

Parameters	Value
Swarm size	100
Learning factor	$c_1 = c_2 = 2.0$
Maximum velocity	500 meters/iteration
Maximum size of personal best solution set	32
Maximum size of global best solution set	70

Table 6
C-metric values.

	s_1	s_2	s_3	s_4	s_5	s_6	s_7	s_8	s_9	s_{10}	s_{11}	s_{12}	s_{13}	s_{14}	s_{15}	s_{16}
s_1	1.00	0.97	0.97	0.97	0.70	0.74	0.75	0.75	0.77	0.78	0.78	0.78	0.84	0.84	0.84	0.84
s_2	1.00	1.00	1.00	1.00	0.73	0.77	0.77	0.77	0.78	0.79	0.79	0.79	0.87	0.87	0.87	0.87
s_3	1.00	1.00	1.00	1.00	0.73	0.77	0.77	0.77	0.78	0.79	0.79	0.79	0.87	0.87	0.87	0.87
s_4	1.00	1.00	1.00	1.00	0.73	0.77	0.77	0.77	0.78	0.79	0.79	0.79	0.87	0.87	0.87	0.87
s_5	0.85	0.86	0.86	0.86	1.00	1.00	1.00	1.00	0.82	0.82	0.82	0.82	0.95	0.95	0.95	0.95
s_6	0.80	0.81	0.80	0.80	1.00	1.00	1.00	1.00	0.80	0.76	0.76	0.76	0.89	0.89	0.89	0.89
s_7	0.80	0.81	0.80	0.80	1.00	1.00	1.00	1.00	0.80	0.76	0.76	0.76	0.89	0.89	0.89	0.89
s_8	0.80	0.81	0.80	0.80	1.00	1.00	1.00	1.00	0.80	0.76	0.76	0.76	0.89	0.89	0.89	0.89
s_9	0.88	0.89	0.89	0.89	0.97	0.97	0.97	0.97	1.00	1.00	1.00	1.00	0.95	0.95	0.95	0.95
s_{10}	0.88	0.89	0.89	0.89	0.97	0.97	0.97	0.97	1.00	1.00	1.00	1.00	0.95	0.95	0.95	0.95
s_{11}	0.88	0.89	0.89	0.89	0.97	0.97	0.97	0.97	1.00	1.00	1.00	1.00	0.95	0.95	0.95	0.95
s_{12}	0.88	0.89	0.89	0.89	0.97	0.97	0.97	0.97	1.00	1.00	1.00	1.00	0.95	0.95	0.95	0.95
s_{13}	0.90	0.90	0.91	0.91	0.95	0.96	0.96	0.96	0.87	0.85	0.85	0.85	1.00	1.00	1.00	1.00
s_{14}	0.90	0.90	0.91	0.91	0.95	0.96	0.96	0.96	0.87	0.85	0.85	0.85	1.00	1.00	1.00	1.00
s_{15}	0.90	0.90	0.91	0.91	0.95	0.96	0.96	0.96	0.87	0.85	0.85	0.85	1.00	1.00	1.00	1.00
s_{16}	0.90	0.90	0.91	0.91	0.95	0.96	0.96	0.96	0.87	0.85	0.85	0.85	1.00	1.00	1.00	1.00

Table 8
Objective weights.

Scenario no.	Scenario 1	Scenario 2	Scenario 3	Scenario 4
Obj1: Vegetation destruction	0.8	0.1	0.1	0.3
Obj2: Soil erosion	0.1	0.8	0.1	0.3
Obj3: Costs	0.1	0.1	0.8	0.4

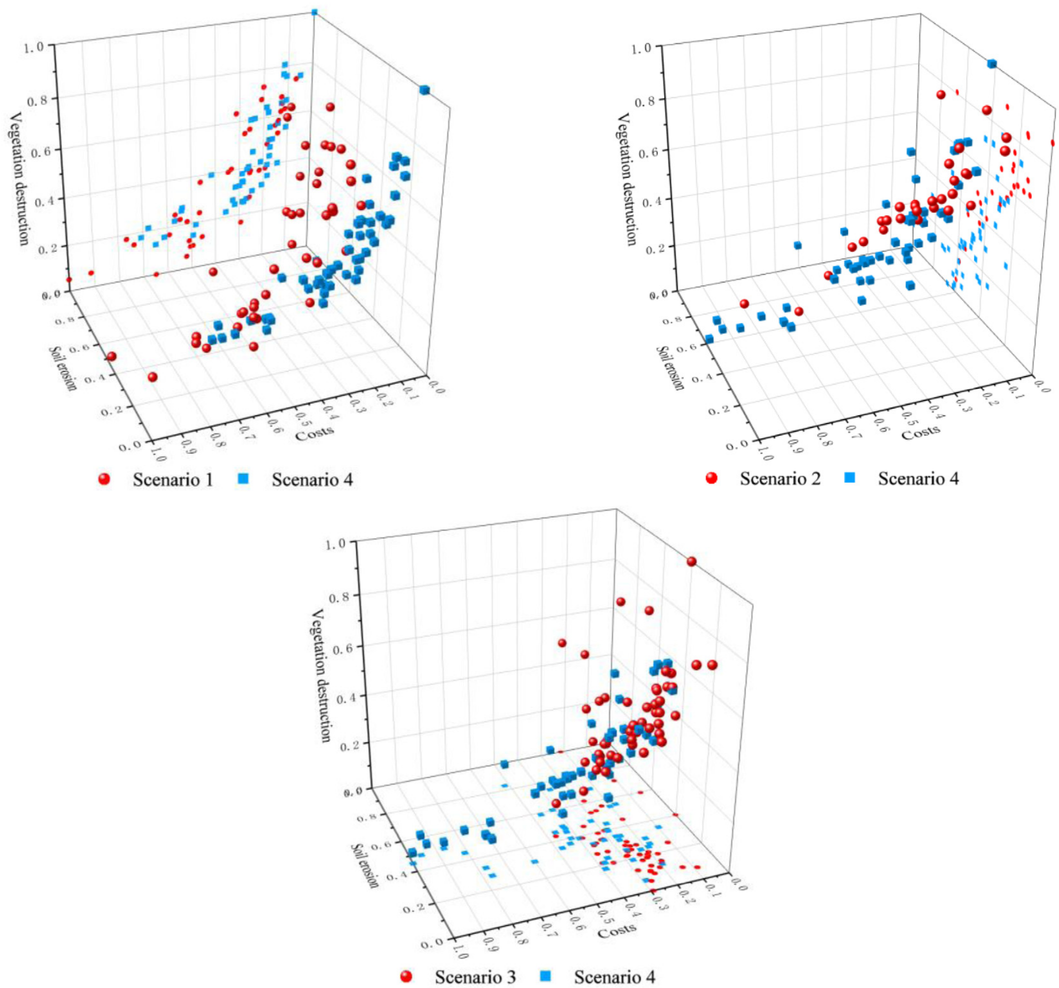

Fig. 12. Comparison of the post-processed Pareto-optimal Fronts.

By inspecting Fig. 13, it can be found that all the pre-specified forbidden zones are bypassed, which demonstrates the effectiveness of the local repair algorithm (LRA).

By reviewing the results of the four alternatives it can be observed that: (1) When the weight of vegetation destruction is highest, the tunnel length of the selected alignment (i.e., Alt 1) is the greatest; (2) When the weight of soil erosion is highest, the bridge length of the selected alignment (i.e., Alt 2) is the greatest; (3) When the weight of cost is highest, the length of cut and fill sections of the selected alignment (i.e., Alt 3) is the greatest; (4) When the weights of the three objectives are similar, the objective function values of the selected best alignment (i.e., Alt 4) are intermediate among these four alternatives. The conflicts among the three objectives considered in this study are analyzed as follows:

The fill sections, cut sections, bridges, and tunnels are the four major structures types of a railway alignment. These four structures types have different impacts on the objectives considered in this study.

(1) The construction costs of fill and cut sections are the lowest. However, serious vegetation damage and soil erosion result if the alignment traverses in the form of fill and cut sections.

(2) The levels of vegetation destruction and soil erosion are much lower if the alignment traverses in the form of bridges. However, the construction costs are higher for bridges than for fill sections when the alignment is close to the terrain surface. Also, the maximum allowable pier height is limited by the current construction technology. This constraint must be satisfied.

(3) The construction costs for tunnels are also higher than for cut sections unless the tunnels are far below the terrain surface. Moreover, building tunnels would produce a vast amount of spoil, which would cause soil erosion. However, the vegetation is not damaged if the alignment traverses in the form of tunnels.

Therefore, if we focus on the economic objective of reducing the costs, the alignment should traverse in the form of relatively shallow fill and cut sections as much as possible. The obtained result of Scenario 3 (i.e., Alt 3) illustrates this point. If soil and water conservation is the main objective, fill and cut sections as well as tunnels are not preferred. The alignment optimization algorithm should try to find suitable areas for traversing in the form of bridges. This point is illustrated by the obtained result of Scenario 2 (i.e., Alt 2). If we focus on protecting the vegetation, the alignment should traverse in the form of bridges and tunnels

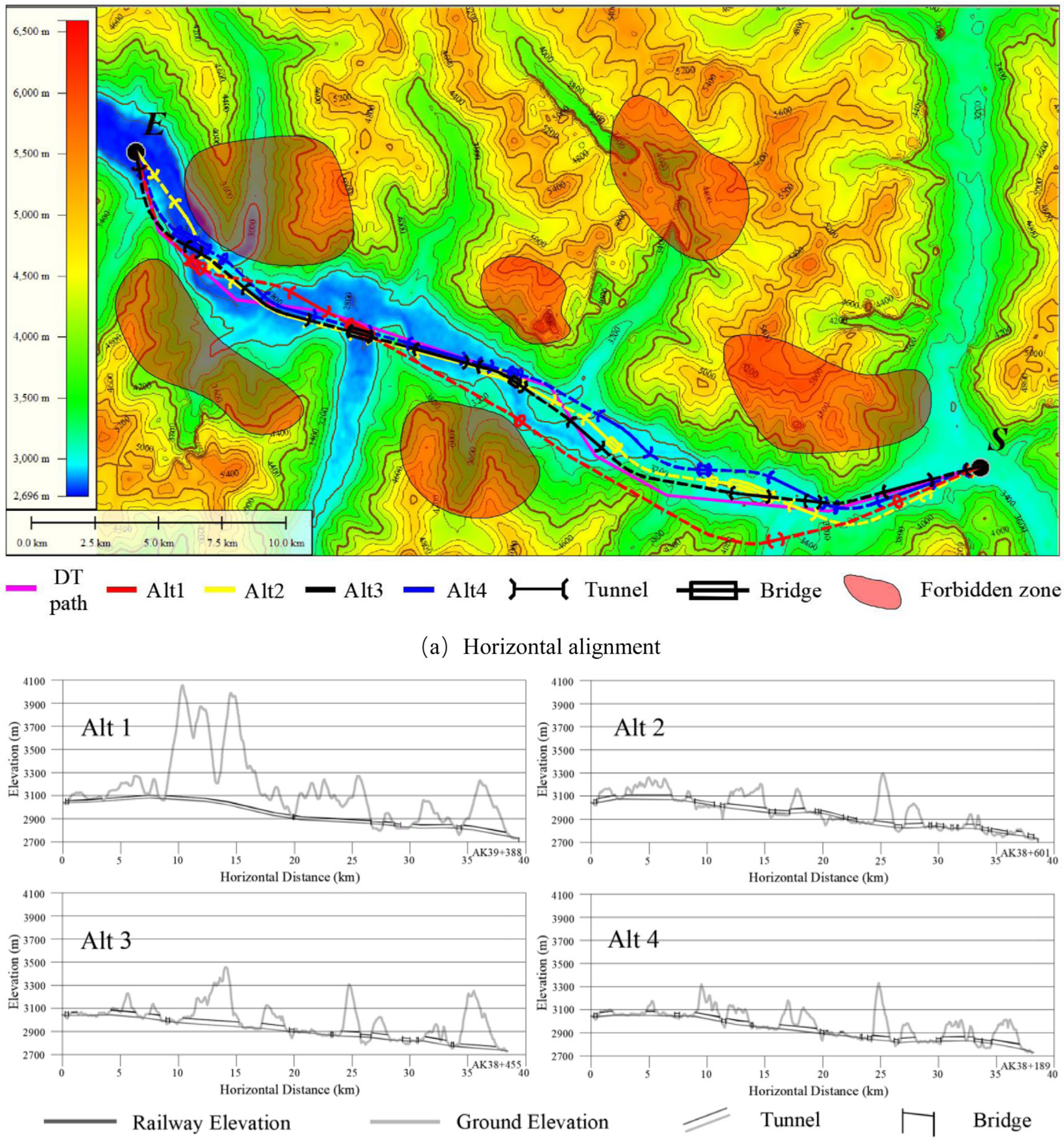

(a) Horizontal alignment

(b) Vertical alignment

Fig. 13. Horizontal and vertical alignments of Alt 1, Alt 2, Alt 3, and Alt 4.

Table 9
Detailed results for Alt 1, Alt 2, Alt 3, and Alt 4.

	Vegetation destruction (NDVI)	Soil erosion (m^3)	Annual costs (million ¥)	Subgrade length (m)	Bridge length (m)	Tunnel length (m)
Alt1	77.08	5,068,425	159.647	3,361	2,442	33,585
Alt2	169.71	3,585,596	126.575	9,125	11,094	18,382
Alt3	210.08	4,392,906	118.621	12,573	3,014	22,868
Alt4	205.52	4,295,591	121.395	11,149	4,186	22,854

as much as possible. However, since the maximum allowable pier height is limited, it would be difficult to find suitable regions to build bridges, especially in complex mountainous regions as this railway case. Thus, tunnels could be the major structure type of the optimized alignment, which could be very different than an alignment whose major structure types are bridges or earthwork segments. The obtained result of Scenario 1 (i.e., Alt 1) illustrates this point.

The aforementioned results and analyses demonstrate that the proposed method can optimize the alignment according to the objective weights and generate alignments which bypass the forbidden zones.

5.2. The second railway case

We apply the developed multi-objective optimization method to solve another railway case which is larger than the first and compare the results with those obtained using the single-objective optimization method developed in our previous work [3]. The developed methods in this study and our previous work are termed MPSO and SPSO, respectively.

This railway case is a Grade I railway, from Maoxian (3506944.120, 35390718.808, 1508.91) to Taiping (3556583.808, 35380569.235, 2275.204). The airline distance between the start

Table 10
MPSO generated best alignment compared with SPSO generated best alignment.

	Elapsed time (min)	Vegetation destruction (NDVI)	Soil erosion (m^3)	Annual costs (million ¥)
SPSO generated best alignment	85	251.940	14,154,661	166.097
MPSO generated best alignment	134	118.216	9,870,895	221.491

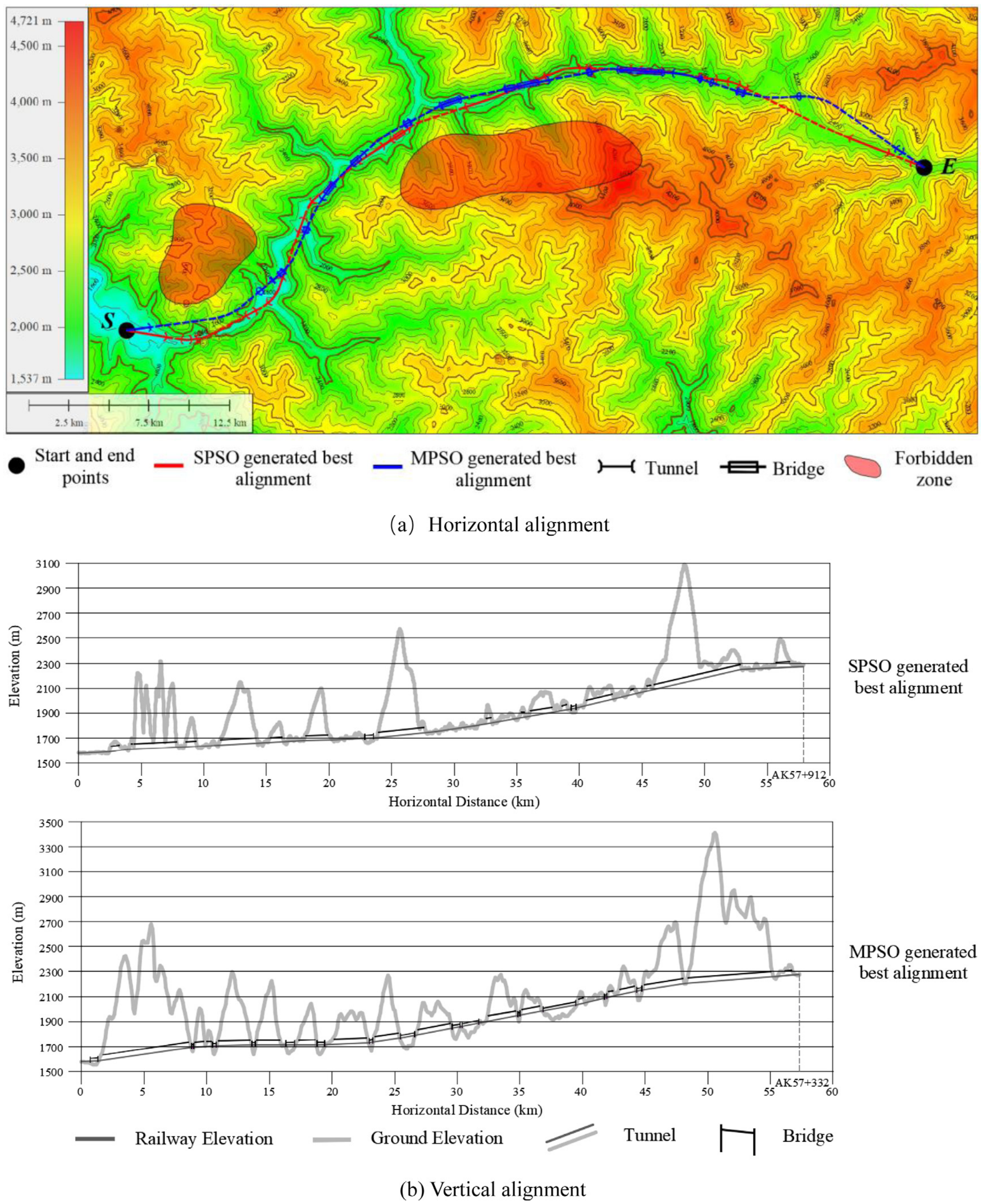

Fig. 14. Comparing the alignments generated with MPSO and SPSO.

and end points is 50656.222 m. The 1512 sq. kilometers (56 km×27 km) study area is represented with 1867 × 900 rectangular lattice cells (30 m × 30 m). There are two forbidden zones in this region. The weight of the costs, soil erosion, and vegetation destruction is set as 0.4, 0.3, 0.3, respectively. Other parameters, including unit costs, railway major technical parameters, constraint parameters, and PSO parameters, are set equal to those in the first railway case.

The program also runs on the HP Z600 workstation (Intel Xeon E5506 2.13 G processor, 4 GB RAM, 500 GB Hard disk). The elapsed time of MPSO is 134 min. A total of seventy non-dominated solutions are generated. According to the objective weights, we select the best alignment from the non-dominated solution set by Eq. (24) and compare with the best alignment which is generated using SPSO, as shown in Table 10 and Fig. 14.

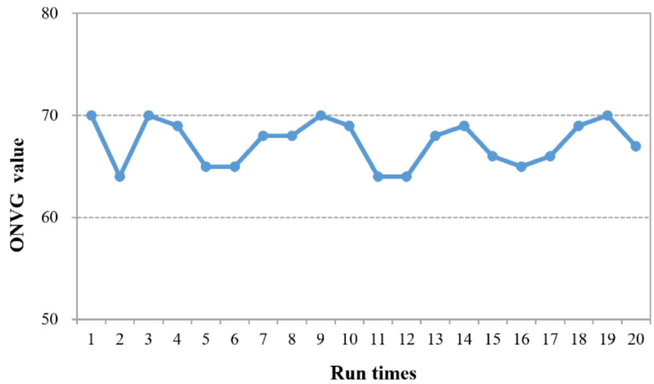

Fig. 15. ONVG values for 20 independent runs.

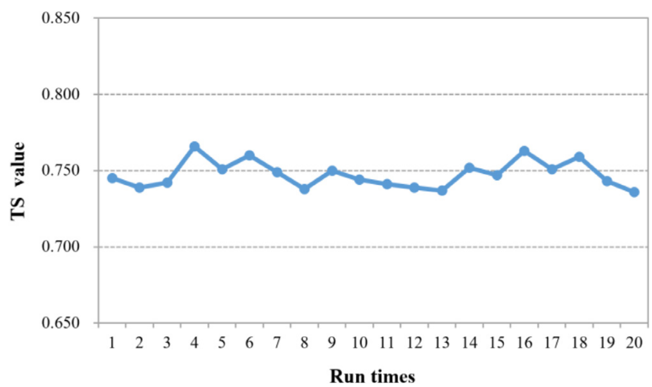

Fig. 16. TS values of the 20 independent runs.

By reviewing the results, it can be observed that the computation time is greater for MPSO than SPSO. This is because finding the personal best and global best solutions from a number of non-dominated solutions takes time, while for the single optimization problem, the personal best and global best solutions can be directly determined. Besides, as SPSO does not consider the soil erosion and vegetation destruction, it also saves time. However, the best alignment generated using MPSO is more eco-friendly. As pointed in the introduction, besides the costs, the environmental impacts are also important factors in designing the railway alignment, especially in mountainous regions where the natural environment is fragile. Therefore, though MPSO requires more computation time, the generated alignment alternative could be preferable.

5.3. Robustness of the method

We further test the robustness of the developed method through the railway case from Maoxian to Taiping. The weight of the three optimization objectives (i.e., costs, soil erosion, and vegetation destruction) is set as 0.4, 0.3, 0.3, respectively. We execute the program 20 independent times and analyze the robustness of the method from the following three aspects:

(1) Number of non-dominated solutions

The number of non-dominated solutions, which is defined as non-dominated vector generation (ONVG) [37], is an indicator for assessing the performance of a multi-optimization algorithm. A larger value of ONVG means that the algorithm is able to output more options for the decision maker and thus is preferable. According to the optimization results, the ONVG value of the non-dominated solution set obtained in each independent run changes slightly, as shown in Fig. 15.

(2) Uniformity of the non-dominated solution set

Uniformity is also an indicator which can assess the performance of a multi-optimization algorithm. We introduce the Tan's Spacing (TS) metric [37] to measure the uniformity and compare the non-dominated solution sets of the 20 independent runs through the TS values. The TS value is calculated with Eqs. (25)

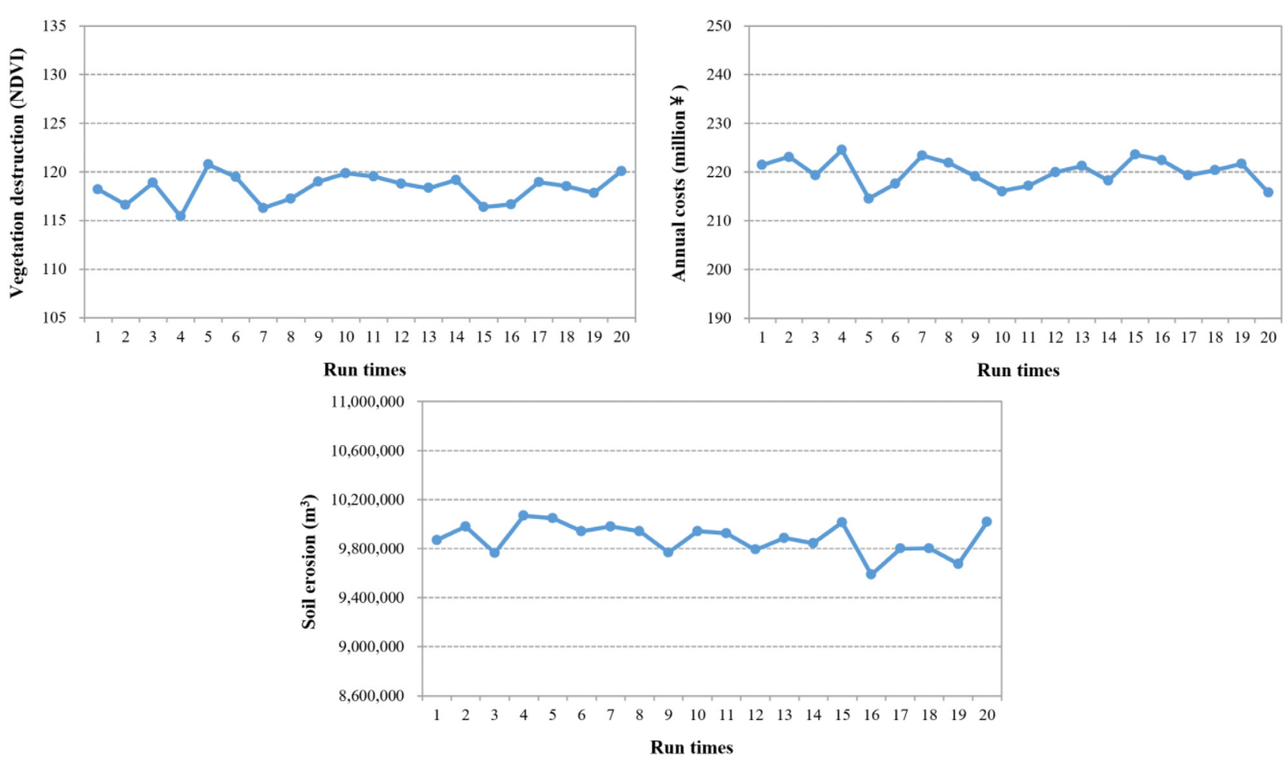

Fig. 17. Objective function values of the 20 selected alignments.

and (26):

$$TS(j) = \frac{1}{\overline{D}} \sqrt{\frac{1}{|S_j|} \sum_{i=1}^{|S_j|} (D_i - \overline{D})^2} \tag{25}$$

$$\overline{D} = \frac{1}{|S_j|} \sum_{i=1}^{|S_j|} D_i \tag{26}$$

where S_j is the obtained non-dominated solution set in the *jth* independent run, $TS(j)$ is the TS value of S_j, $|S_j|$ is the number of solutions in S_j, D_i is the Euclidean distance in the objective space between the *ith* solution and its nearest neighbor in S_j. The smaller the TS value is, the more evenly the solutions in S_j are distributed. The TS values of the solutions obtained in the 20 independent runs are shown in Fig. 16.

Fig. 16 shows that the TS values of the non-dominated solution sets obtained in the 20 independent runs are very close.

(3) The best non-dominated solution according to the objective weights

According to the weights of the three objectives, we select the best alignment from each non-dominated solution set and compare the objective function values of the 20 selected solutions, as shown in Fig. 17.

From Fig. 17, we can see that the fluctuations of the three objective function values are all within 5%.

By reviewing Fig. 15, 16, and 17 it can be observed that the optimization results obtained in the 20 independent runs are very stable, which shows the robustness of the developed method.

6. Conclusions

This paper developed a method for railway alignment optimization which can optimize costs and environmental impacts of a railway simultaneously. An optimization model containing vegetation destruction, soil erosion, construction cost, and operating cost was formulated. To solve the optimization model, a PSO-based multi-objective optimization method with a local repair algorithm was proposed. The main improvements of the developed method are summarized as follows:

1. For the optimization model, two new quantitative indexes for measuring the environmental impacts caused by railway construction were proposed. One index reflects the vegetation destruction. The NDVI, which is widely used for remote sensing of vegetation, was introduced to evaluate the damage to vegetation. The other index, which is quantified as the spoil volume, was defined to indicate the soil erosion. The spoil volume was used here as a proxy variable for soil erosion. Compared with previous quantitative indexes, the new indexes can measure the environmental impacts more accurately.

2. For the optimization method, three novel functions for dealing with the multi-objective optimization model were proposed, including an MTD-based update mechanism of personal best solution, a global best solution update mechanism based on objective function values and crowding value, as well as a local repair algorithm (LRA). The LRA is based on a customized crossover operator and intended to save promising alignment alternatives during the search process.

The method has been applied to two real-world railway cases. The results indicate that the developed method can trade off the economic and environmental objectives according to different weights specified by the designers generating trade-off solutions which bypass the forbidden zones. Compared with the single-objective PSO algorithm, a more eco-friendly as well as balanced alignment alternative can be found according to the designers' preference information.

In this study, we mainly considered the environmental impacts during the railway construction stage. The railway will also affect its surrounding environment during its operating life. Future studies will consider environmental impacts due to railway presence and operation as well as other factors, such as potential traffic demand, safety, and connections with existing roads or railways.

Declaration of competing interest

No author associated with this paper has disclosed any potential or pertinent conflicts which may be perceived to have impending conflict with this work. For full disclosure statements refer to https://doi.org/10.1016/j.asoc.2020.106105.

CRediT authorship contribution statement

Hong Zhang: Methodology, Writing - original draft, Writing - review & editing. **Hao Pu:** Funding acquisition, Project administration, Supervision. **Paul Schonfeld:** Methodology, Writing - review & editing. **Taoran Song:** Software, Validation. **Wei Li:** Investigation, Validation. **Jie Wang:** Data curation, Resources. **Xianbao Peng:** Data curation, Resources. **Jianping Hu:** Data curation, Resources.

Acknowledgments

This work was supported by the National Science Foundation China (NSFC) [grant numbers 51778640, 51608543, and 51678574], the National Key R&D Program of China with award number 2017YFB1201102, Project of Science and Technology Research and Development Plan of China National Railway Group Co. Ltd with award number P2019G003. The authors are very grateful to China Railway First Survey and Design Institute Group Co. Ltd, China Railway Eryuan Engineering Group CO.LTD, and China Railway Siyuan Survey and Design Group Co., LTD for supporting us with many real cases.

Appendix

Mechanism1: Personal best solution determining mechanism

Input: The personal best solution set of the *ith* particle $\boldsymbol{\Phi}_i$

Output: The personal best solution

$N_p \leftarrow$ Number of non-dominated solutions in $\boldsymbol{\Phi}_i$
$N_o \leftarrow$ Number of objective functions
for $a \leftarrow 0$ **to** N_p, **do**
  for $j \leftarrow 0$ **to** N_o, **do**
    for $b \leftarrow 0$ **to** N_p, **do**
      if $f^{(j)}(a) \geq f^{(j)}(b)$ **then**
        $t^{(j)}(a,b) = 0$
      if $f^{(j)}(a) < f^{(j)}(b)$ **then**
        $t^{(j)}(a,b) = 1$
      end if
    end for
    $T^{(j)}(a, \boldsymbol{\Phi}_i) = \sum_{\forall b \in \Phi_i \wedge a \neq b} \frac{t^{(j)}(a,b)}{(|\boldsymbol{\Phi}_i| - 1)}$
  end for
  $R(a) = \sum_{j=1}^{N_o} w_j \cdot T^{(j)}(a, \boldsymbol{\Phi}_i)$
end for
R $\leftarrow$ sort[a, $R(a)$] // Sort in descending using $R(a)$
$S \leftarrow$ the best ranked solution
return S

Mechanism2: Global best solution determining mechanism

Input: The global best solution set $\mathbf{\Phi}$

Output: The global best solution

$N_g \leftarrow$ Number of non-dominated solutions in $\mathbf{\Phi}$
$N_o \leftarrow$ Number of objective functions
$f_{\max}^{(j)}(\mathbf{\Phi}) \leftarrow$ The maximum value of the *jth* objective function of all the solutions in $\mathbf{\Phi}$
$f_{\min}^{(j)}(\mathbf{\Phi}) \leftarrow$ The minimum value of the *jth* objective function of all the solutions in $\mathbf{\Phi}$
for $a \leftarrow 0$ **to** N_g, **do**
  for $b \leftarrow 0$ **to** N_p, **do**
    for $j \leftarrow 0$ **to** N_o, **do**
      $d^{(j)}(a,b) = \dfrac{f^{(j)}(a) - f^{(j)}(b)}{f_{\max}^{(j)}(\mathbf{\Phi}) - f_{\min}^{(j)}(\mathbf{\Phi})}$
    end for
    $D(a,b) = \sqrt{\sum_{j=1}^{N_o} d^{(j)}(a,b)^2}$
  end for
  $R \leftarrow$ sort[a, $D(a, b)$] // Sort in ascending using $D(a, b)$
  $\rho_a = \dfrac{1}{\left((1/k)\sum_{r=1}^{k} D_a^{(r)}\right)}$ // calculate the crowding value
end for
$R1 \leftarrow$ sort[a, ρ_a] // Sort in ascending using ρ_a
for $a \leftarrow 0$ **to** N_g, **do**
  for $j \leftarrow 0$ **to** N_o, **do**
    for $b \leftarrow 0$ **to** N_g, **do**
      if $f^{(j)}(a) \geq f^{(j)}(b)$ **then**
        $t^{(j)}(a,b) = 0$
      if $f^{(j)}(a) < f^{(j)}(b)$ **then**
        $t^{(j)}(a,b) = 1$
      end if
    end for
    $T^{(j)}(a,\mathbf{\Phi}_i) = \sum_{\forall b \in \Phi_i \wedge a \neq b} \dfrac{t^{(j)}(a,b)}{(|\mathbf{\Phi}_i| - 1)}$
  end for
  $R(a) = \sum_{j=1}^{N_o} w_j \cdot T^{(j)}(a,\mathbf{\Phi}_i)$
end for
$R2 \leftarrow$ sort[a, $R(a)$] // Sort in descending using $R(a)$
for $a \leftarrow 0$ **to** N_g, **do**
  $P_a = \dfrac{2(|\mathbf{\Phi}|+1) - R1_a - R2_a}{|\mathbf{\Phi}|(|\mathbf{\Phi}|+1)}$
end for
$S \leftarrow$ the solution with the maximum P_a value
return S

References

[1] S. Samanta, M.K. Jha, Modeling a rail transit alignment considering different objectives, Transp. Res. A 45 (1) (2011) 31–45.

[2] W. Li, H. Pu, P. Schonfeld, H. Zhang, X. Zheng, Methodology for optimizing constrained 3-dimensional railway alignments in mountainous terrain, Transp. Res. C 68 (2016) 549–565.

[3] H. Pu, T. Song, P. Schonfeld, W. Li, H. Zhang, J. Hu, X. Peng, J. Wang, Mountain railway alignment optimization using stepwise & hybrid particle swarm optimization incorporating genetic operators, Appl. Soft Comput. 78 (2019) 41–57.

[4] D.A. Hirpa, Simultaneous Optimization of Vertical and Horizontal Road Alignments (M.S. dissertation), University of British Columbia, Okanagan, 2014.

[5] J.C. Jong, Optimizing Highway Alignments with Genetic Algorithms (Ph.D. dissertation), University of Maryland, College Park, 1998.

[6] E. Kim, M.K. Jha, B. Son, Improving the computational efficiency of highway alignment optimization models through a stepwise genetic algorithms approach, Transp. Res. B 39 (4) (2005) 339–360.

[7] M. Kang, P. Schonfeld, N. Yang, Prescreening and repairing in a genetic algorithm for highway alignment optimization, Comput.-Aided Civ. Infrastruct. Eng. 24 (2) (2009) 109–119.

[8] X.R. Lai, Optimization of Station Locations and Track Alignments for Rail Transit Lines (Ph.D. dissertation), University of Maryland, College Park, 2012.

[9] N. Davey, S. Dunstall, S. Halgamuge, Optimal road design through ecologically sensitive areas considering animal migration dynamics, Transp. Res. C 77 (2017) 478–494.

[10] R. Babapour, R. Naghdi, I. Ghajar, Z. Mortazavi, Forest road profile optimization using meta-heuristic techniques, Appl. Soft Comput. 64 (2018) 126–137.

[11] A.L. Costa, M.C. Cunha, P.A.L.F. Coelho, H.H. Einstein, Solving high-speed rail planning with the simulated annealing algorithm, J. Transp. Eng. 139 (6) (2013) 635–642.

[12] A.L. Costa, M.C. Cunha, P.A.L.F. Coelho, H.H. Einstein, Decision support systems for real-world high-speed rail planning, J. Transp. Eng. 142 (5) (2016) 04016015.

[13] W. Hare, S. Hossain, Y. Lucet, F. Rahman, Models and strategies for efficiently determining an optimal vertical alignment of roads, Comput. Oper. Res. 44 (2014) 161–173.

[14] W. Hare, Y. Lucet, F. Rahman, A mixed-integer linear programming model to optimize the vertical alignment considering blocks and side-slopes in road construction, European J. Oper. Res. 241 (3) (2015) 631–641.

[15] S. Mondal, Y. Lucet, W. Hare, Optimizing horizontal alignment of roads in a specified corridor, Comput. Oper. Res. 64 (2015) 130–138.

[16] D. Hirpa, W. Hare, Y. Lucet, Y. Pushak, S. Tesfamariam, A bi-objective optimization framework for three-dimensional road alignment design, Transp. Res. C 65 (2016) 61–78.

[17] Y. Pushak, W. Hare, Y. Lucet, Multiple-path selection for new highway alignments using discrete algorithms, European J. Oper. Res. 248 (2) (2016) 415–427.

[18] W. Li, H. Pu, P. Schonfeld, J. Yang, H. Zhang, L. Wang, J. Xiong, Mountain railway alignment optimization with bidirectional distance transform and genetic algorithm, Comput.-Aided Civ. Infrastruct. Eng. 32 (8) (2017) 691–709.

[19] H. Pu, H. Zhang, W. Li, J. Xiong, J. Hu, J. Wang, Concurrent optimization of mountain railway alignment and station locations using a distance transform algorithm, Comput. Ind. Eng. 127 (2019) 1297–1314.

[20] H. Pu, T. Song, P. Schonfeld, W. Li, H. Zhang, J. Wang, X. Peng, A three-dimensional distance transform for optimizing constrained mountain railway alignments, Comput.-Aided Civ. Infrastruct. Eng. 34 (2019) 972–990.

[21] T. Song, H. Pu, P. Schonfeld, W. Li, H. Zhang, Y. Ren, J. Wang, J. Pu, X. Peng, A parallel three-dimensional distance transform for railway alignment optimization using, OpenMP, J. Transp. Eng. A (2019) http://dx.doi.org/10.1061/JTEPBS.0000344, in press.

[22] A. Maji, M.K. Jha, Multi-objective highway alignment optimization using a genetic algorithm, J. Adv. Transp. 43 (4) (2009) 481–504.

[23] A. Maji, M.K. Jha, A multi-objective analysis of impacted area of environmentally preserved land and alignment cost for sustainable highway infrastructure design, Procedia-Soc. Behav. Sci. 20 (2011) 966–972.

[24] N. Yang, M.W. Kang, P. Schonfeld, M.K. Jha, Multi-objective highway alignment optimization incorporating preference information, Transp. Res. C 40 (2014) 36–48.

[25] R. Eberhart, J. Kennedy, A new optimizer using particle swarm theory, in: Proceedings of the Sixth International Symposium on Micro Machine and Human Science, IEEE, 1995, pp. 39–43.

[26] J. Luo, Y. Qi, J. Xie, X. Zhang, A hybrid multi-objective PSO–EDA algorithm for reservoir flood control operation, Appl. Soft Comput. 34 (2015) 526–538.

[27] W. Deng, H. Zhao, X. Yang, J. Xiong, M. Sun, B. Li, Study on an improved adaptive PSO algorithm for solving multi-objective gate assignment, Appl. Soft Comput. 59 (2017) 288–302.

[28] Y. Shafahi, M. Bagherian, A customized particle swarm method to solve highway alignment optimization problem, Comput.-Aided Civ. Infrastruct. Eng. 28 (1) (2013) 52–67.

[29] Ministry of Railways of People's Republic of China, Code for Environmental Protection Design of Railway Engineering, China Railway Publishing House Co. Ltd, Beijing, 1998 (in Chinese).

[30] S.M. Vicente-Serrano, J.J. Camarero, J.M. Olano, N. Martín-Hernández, M. Peña Gallardo, M. Tomás-Burguera, A. Gazol, C. Azorin-Molina, U. Bhuyan, A.E.V. Kenawy, Diverse relationships between forest growth and the normalized difference vegetation index at a global scale, Remote Sens. Environ. 187 (2016) 14–29.

[31] B.C. Gao, NDWI—A normalized difference water index for remote sensing of vegetation liquid water from space, Remote Sens. Environ. 58 (3) (1996) 257–266.

[32] D. Pimentel, C. Harvey, P. Resosudarmo, K. Sinclair, D. Kurz, M. McNair, S. Crist, L. Shpritz, L. Fitton, R. Saffouri, R. Blair, Environmental and economic costs of soil erosion and conservation benefits, Science 267 (5201) (1995) 1117–1123.

[33] H. Yang, L. Lin, Y. He, Soil erosion caused by highway construction in expansive soils districts and its prevention measures, in: Geotechnical Engineering for Disaster Mitigation and Rehabilitation, Springer, Berlin, Heidelberg, 2008, pp. 781–789.

[34] M.E. Vázquez-Méndez, G. Casal, D. Santamarina, A. Castro, A 3d model for optimizing infrastructure costs in road design, Comput.-Aided Civ. Infrastruct. Eng. 33 (2018) 423–439.

[35] Ministry of Railways of People's Republic of China, Code for Design of Railway Line, China Planning Press, Beijing, 2017 (in Chinese).

[36] W. Li, H. Pu, P. Schonfeld, Z. Song, H. Zhang, L. Wang, J. Wang, X. Peng, L. Peng, A method for automatically recreating the horizontal alignment geometry of existing railways, Comput.-Aided Civ. Infrastruct. Eng. 34 (1) (2019) 71–94.

[37] R. Zhang, P.C. Chang, S. Song, C. Wu, Local search enhanced multi-objective PSO algorithm for scheduling textile production processes with environmental considerations, Appl. Soft Comput. 61 (2017) 447–467.

[38] D. Teodorović, Swarm intelligence systems for transportation engineering: Principles and applications, Transp. Res. C 16 (6) (2008) 651–667.

[39] Y. Shi, R. Eberhart, A modified particle swarm optimizer, in: IEEE International Conference on Evolutionary Computation Proceedings, 1998, pp. 69–73.

[40] H. Pu, H. Zhang, P. Schonfeld, W. Li, J. Wang, X. Peng, J. Hu, Maximum gradient decision-making for railways based on convolutional neural network, J. Transp. Eng. A 145 (11) (2019) 04019047.

[41] R.O. Parreiras, J.A. Vasconcelos, Decision making in multi-objective optimization aided by the multi-criteria tournament decision method, Nonlinear Anal. TMA 71 (12) (2009) e191–e198.

[42] J. Branke, S. Mostaghim, About selecting the personal best in multi-objective particle swarm optimization, in: Parallel Problem Solving from Nature-PPSN IX, Springer, Berlin, Heidelberg, 2006, pp. 523–532.

[43] A. Lipowski, D. Lipowska, Roulette-wheel selection via stochastic acceptance, Physica A 391 (6) (2012) 2193–2196.